Removal of tetracycline from polluted water by chitosan-olive pomace adsorbing films

Removal of tetracycline from polluted water by chitosan-olive pomace adsorbing films

Vito Rizzi[a], Dario Lacalamita[a], Jennifer Gubitosa[b], Paola Fini[b], Andrea Petrella[c], Roberto Romita[a], Angela Agostiano[a,b], José Antonio Gabaldón[d], María Isabel Fortea Gorbe[d], Teresa Gómez-Morte[d] and Pinalysa Cosma[a,b*]

[a]Università degli Studi "Aldo Moro" di Bari, Dip. Chimica, Via Orabona, 4- 70126 Bari, Italy ;

[b]Consiglio Nazionale delle Ricerche CNR-IPCF, UOS Bari, Via Orabona, 4- 70126 Bari, Italy;

[c]Dipartimento di Ingegneria Civile, Ambientale, Edile, del Territorio e di Chimica, Politecnico di Bari, Orabona, 4, 70125, Bari, Italy;

[d]Departamento Ciencia y Tecnología de Alimentos, Universidad Católica San Antonio de Murcia, Guadalupe, Murcia, Spain.

*Prof. Pinalysa COSMA

Università degli Studi "Aldo Moro" di Bari

Dipartimento di Chimica

Via Orabona, 4

I-70126 Bari, ITALY

e-mail: pinalysa.cosma@uniba.it

tel. +39 0805443443

fax +39 0805442128

ABSTRACT

Emerging pollutants are producing significant and negative effects on environmental with impact both on aquatic and land ecosystems. Therefore, this study focusses on the removal of tetracycline, a largely used wide-ranging antibiotic, through adsorption processes, from water by using, for the first time, raw olive solid wastes (olive pomace) and olive solid waste/chitosan blended film. The effects on the adsorption process of pH values, ionic strength, amount of adsorbent and pollutant and temperature values were investigated. Results indicated the presence of electrostatic interaction and H-bonding between the adsorbent and tetracycline. The kinetics, isotherms of adsorption and thermodynamic parameters ($\Delta G°$, $\Delta H°$ and $\Delta S°$) were evaluated observing that the adsorption occurred on heterogeneous surfaces, endothermic and spontaneous, with high percentage of removal. More specifically the 80% of tetracycline was adsorbed, by adopting 3h and 2h as contact time, by raw olive solid waste and blended adsorbent, respectively inferring the following adsorption capacities: 16 $mg \times g^{-1}$ and 1.6 $mg \times g^{-1}$. Despite these relative low adsorption capacities, experiments of desorption were performed and the 80% of adsorbed tetracycline was recovered proposing a low-cost and cleaner approach of great significance for the recover of pollutant and safe reuse of the adsorbent enabling consecutive cycles of adsorption/desorption, transforming a waste in resource. Additionally, the use of Advanced Oxidation Processes was proposed as possible alternative for the recovery of tetracycline obtaining its degradation after the desorption.

KEYWORDS: olive mill solid wastes, chitosan, emerging pollutants, tetracycline, photodegradation, TiO_2

INTRODUCTION

Among different sources of contamination affecting water, the use of antibiotics is becoming an important global concern (Dehgan et al, 2019). Indeed, antibiotics are largely employed to treat several diseases induced by bacterial or pathogenic microbes bringing to their accumulation in the environment that are getting worse the problem (Xiaofeng et al., 2019). Accordingly, in the recent years, the number of publications regarding the detection and the removal of pharmaceuticals and personal care products from aquatic environment, is increasing (Sophia and Lima,2018) stressing the emergency related to emerging pollutants (EPs) removal from water (Naidu et al. 2016). Among EPs, tetracycline (TC), a broad-spectrum antibiotic usually applied in human and veterinary medicine (Chen et al.,2016) to treat infectious diseases, is frequently retrieved in wastewater (Yeşilova et al.,2018; Safari et al., 2015; Martins et al.,2015; Zhu et al.,2014). TC is hardly degraded for its antibacterial broad spectrum and stable naphthalene structure. Further, only a small portion of TC can be degraded to inactive products through metabolic reactions such as basification, dissociation, and glucuronidation. Most of them retain their toxicity to soil and water as prototypes or metabolites (Dai et al., 2019). Adverse effects on ecosystems and human health, as allergies and antibiotic resistance are reported by Chen et al. (2016). As a result, with the increasing concern for water quality and public health, the development of efficient platforms for TC removal from water is highly desirable, by applying new efficient, sustainable and low-cost wastewater treatment technologies avoiding the direct degradation of the pollutant in water. Among various approaches, the adsorption methods are considered the most powerful tools for wastewater treatment, avoiding the release of secondary pollutants (Martins et al., 2015), being an efficient and low-cost

approach, requiring easy operation for holding pollutants, appearing also as a highly versatile technique (Martins et al.,2015; Ahmed and Hameed,2018). For example, Selmi et al.(2018) reported the TC removal by using activated carbons from Agave americana fibres and mimosa tannin. The luminescent MOF use was proposed by Zhou et al. (2018). Cryogels for the selective TC removal were described by Yeşilova et al. (2018). Zeolite-hydroxyapatite-activated oil palm ash composite, active carbon and pumice stone were also investigated (Khandaya and Hameed,2018; Fan et al.,2016; Guler and Sarioglu,2014). The importance of the TC removal arises from the very recent publications reported by Dai et al. (2019), Dehghan et al. (2019) and Xiaofeng et al. (2019) that described the use of ground spent coffee, zeolitic imidazolate frameworks and bentonite-derived mesoporous materials for the TC removal. Other interesting results are reported in literature by Zhang et al.,2018; Ahsan et al, 2018; Gao et al. 2012; Ma et al. 2017; Qin. et al. 2018; Sayğılı and Güzel 2016; Zhanga et al. 2015. Among these adsorbents, materials having multiple advantages, proposing the possibility to remove the TC both under dynamic and static condition, recover and reuse the adsorbent for several cycles avoiding the formation of secondary pollutants in water are not presented. On this ground, the present work reports the first example about the development of a cleaner production-pollution prevention approach (Belayutham et al.,2016) by using agricultural wastes for removing TC from water. More specifically, olive pomace (OP), and chitosan membrane (CH) blended with OP (CH/OP) are described. CH was used as physical platform to sustain OP avoiding its dispersion in water for safety applications. Accordingly, in the growing interest towards a cleaner production/sustainability approach in several application fields (Lu et al.,2018; Zilouei et al.,2018; Rizzi et al.,2018a, 2018b, 2016a,2016b; Gubitosa et. al, 2018, Petrella et al, 2010), including environmental technologies, the use of agricultural wastes and chitosan-based adsorbents are appearing very interesting (Liu et al., 2012; Zilouei et

al.,2018, Rizzi et al.,2014; Semeraro et al.,2017; Rizzi et al.,2017a). It is worth to mention that the use OP could be considered as a way for a sustainable cycle, based on the use of wastes (Finnveden et al.,2005; Morali et al.,2016) for cleaner technologies. (Hens et al.,2018). The design aims to reduce the overall environmental impact of products through use of a life-cycle perspective. (Kurk and Eagan, 2008). Moreover, it is noteworthy that OP was previously used to remove textile dyes and metals from water (Rizzi et al.,2017a, 2017b, 2017c; Petrella et al.,2018; Petrella et al.,2017), demonstrating a possible solution to olive mill pollution increasing. During this work, differences between OP and CH/OP were checked on the removal of TC, and CH/OP was selected as the most suitable one, resulting a highly performant low-cost alternative material. A scaling up in the use of pomace blended into chitosan matrix is also presented, performing experiments of adsorption both *in batch* and *in flux*. Other EPs such as ketoprofen, diclofenac, and chlorpyrifos were investigated, discussing as CH/OP was able to efficiently remove another EPs class wide ranging its applications. The TC recover from the adsorbent was also successfully explored proposing the recycle of both adsorbent and TC in a virtuous life-cycle. Advanced Oxidation Processes (AOPs) were proposed as alternative with respect the TC recovery. For this purpose, TiO_2 was directly blended inside the adsorbent obtaining CH/OP/TiO_2 and experiments of solid state TC photodegradation were attempted along with those obtained after the recovery of TC, thus in water, but, far from the purified water. In this way, the harmful photoinduced by products cannot pollute the purified water. The results of this research cannot only make the waste a resource, but also suggest novel approaches for the clearness of water containing TC, that can be of great practical significance.

EXPERIMENTAL

Chemicals. Commercial grade chitosan powder (from crab shells, highly viscous, with deacetylation degree ≥ 75%), Acetic acid (99,9 %) and glycerol (+99.5%) were purchased from Sigma-Aldrich. ^{1}H-NMR (700 MHz) and FTIR-ATR results were agreed between them giving us a deacetylation degree around 70 % confirming the manufacturer's Sigma Aldrich specification. The same commercial source was adopted for Tetracycline (TC: $C_{22}H_{25}N_2O_8$ Cl, M.W. 480,9 g/mol) used without further purification. TC stock solution with a concentration of 1.0×10^{-3} M was prepared. The pH of the various aqueous solutions, when necessary, was adjusted using concentrated HCl and NaOH solutions. Dilutions were performed using deionized water. Aeroxide TiO_2 P25 was gifted from Evonik industries AG. The biosorbent, Olive pomace (OP), was the solid waste of olive oil production, provided from a local oil industry, Bari, Puglia (South of Italy).

In batch equilibrium experiments. Experiments were carried out to study the behavior of OP and CH/OP respect to the TC adsorption. The adsorption capacities were calculated in terms of q_t (mg×g^{-1}) at time *t* for TC, by applying the following **Equation 1** (Rizzi et al.,2017a,2017b,2017c):

$$q_t = \frac{C_0 - C_t}{W} \times V \qquad \textbf{(1)}$$

where *V* represents the volume of adsorbed solution (15mL), *W* is the weight of the dried adsorbent material (g), C_0 and C_t (mg×L^{-1}) represent the concentration of TC at initial and *t* time. In detail, a fixed amount of adsorbent into flasks containing 15 mL of TC solution at different initial concentrations (5.0×10^{-5}M, 2.5×10^{-5}M, 1.25×10^{-5}M, corresponding to 24mg/L, 12mg/L and 6mg/L of TC, respectively) was used. The

adsorbents were put in flasks containing TC solutions, under continuous stirring at 250 rpm, and UV-Vis absorption spectra were recorded to evaluate the TC removal efficiency from water. To infer the exact TC concentration, the internal standard calibration method was used. The effect of both solution ionic strength, (by using different salts at 0.1M and 2M of concentration), and changes in pH values, (ranging from 2 to 12), were also investigated.

Besides, the effect of adsorbent amount was explored as follows:

a) OP: from 6mg to 100mg

b) CH/OP composite films: from 75,14 to 468,87mg (in detail CH/OP1: 75.14; CH/OP2: 173.72mg; CH/OP3: 291.94mg; CH/OP4: 468.87mg).

In batch **desorption experiments.** After the TC adsorption from water, the adsorbent was taken in contact with solutions having high ionic strength. In particular $MgCl_2$ 2M was selected as the best salts to be able to induce the release of the adsorbed TC. With the same approach adopted for the adsorption of TC, the UV-Vis investigation was used to assess the amount of the desorbed pollutant. In detail, after the TC adsorption the adsorbent was washed with fresh water to remove the not adsorbed TC, and swollen in the solution for the release. It is worth to mention that in $MgCl_2$ the following molar absorption coefficient (ε) was used: 17200 M^{-1} cm^{-1}.

In flow **adsorption/desorption experiments.** Among CH/OP and OP, the attention was focused on the use of CH/OP blended films. In particular, the adsorbent was placed inside a commercial syringe-like column 3.00 cm × 5.00 cm and then was swollen with water. Subsequently, solutions of TC having different concentrations slowly flowed (3 mL/min) through the column and the eluting solutions were collected and studied by UV-Vis spectroscopy. When the released of the TC was studied, a 2M $MgCl_2$ solution,

after the adsorption of TC, was flowed through the column and UV-Vis investigation was used to assess the amount of the desorbed TC.

For instrumental details and procedure for the adsorbents preparation see ESI.

Adsorption kinetics. In order to obtain information related to the kinetics of the adsorption process, both pseudo-first-order and pseudo-second-order kinetic models were adopted and applied to experimental data. The linearized equations for pseudo-first (**Equation 2**) and pseudo-second-order (**Equation 3**) models were adopted (Rizzi et al.,2017a):

$$\ln(q_e - q_t) = \ln(q_e) - K_1 \times t \quad \textbf{(2)}$$

$$\frac{t}{q_t} = \frac{1}{K_2 q_e^2} + \frac{1}{q_e} \times t \quad \textbf{(3)}$$

where q_e and q_t represent the OP or CH/OP adsorption capacities at equilibrium and at time *t*, respectively ($mg \times g^{-1}$) and k_1 (min^{-1}) and k_2 ($g \times (mg \times min)^{-1}$) are the rate constants of pseudo-first and second order models, respectively.

Swelling ratio measurements for CH/OP. CH/OP in absence and in presence of TC, were subject to swelling ratio measurements. The films were cut to a square piece of 1 cm × 1 cm and immersed in bi-distilled water, at controlled room temperature, and

measurements were performed every minute until the equilibrium was attained. The films were blotted with filter paper and weighed. **Equation 4** was used to determine the swelling ratio percentage (Rizzi et al.,2016a) .

$$Swelling\ ratio\ \% = \frac{W_s - W_d}{W_d} \times 100 \quad \textbf{(4)}$$

where W_s is the weight of the swollen film at time t and W_d is the weight of the dried film (the weight of each film before the contact with water).

Adsorption Isotherms. Among the reported models, the Langmuir, Freundlich and Temkin isotherm equations (Rizzi et al.,2018b) were applied to analyze the sorption process of TC on the presented adsorbents. When the Langmuir model well fit the experimental data, it describes the adsorption on homogeneous surfaces with uniformly energetic adsorption sites and monolayer coverage. The interaction between adsorbed molecules is not predicted. **Equation 5** reports the adopted linear form of the Langmuir equation:

$$\frac{C_e}{q_e} = \frac{1}{K_L Q_0} + \frac{C_e}{Q_0} \quad \textbf{(5)}$$

where q_e ($mg \times g^{-1}$) is the adsorbed amount of TC at equilibrium, C_e is the equilibrium concentration of the TC ($mg \times L^{-1}$) in solution, K_L is Langmuir equilibrium constant ($L \times mg^{-1}$) and Q_0 the maximum adsorption capacity ($mg \times g^{-1}$). The Freundlich isotherm was also applied. The assumption of the model is that the surface of the adsorbent is heterogeneous and adsorption sites having different energy of adsorption are

contemplated. The energy of adsorption varies as a function of the surface coverage. **Equation 6** reports the linear form of this equation.

$$\log(q_e) = \log(K_F) + \frac{1}{n}\log(C_e)$$

(6)

where K_F ($L \times mg^{-1}$) is the Freundlich constant and n is the heterogeneity factor. K_F is related to the adsorption capacity, whereas the 1/n value indicates if the isotherm is irreversible (1/n=0), favorable (0<1/n<1) or unfavorable (1/n>1). When the Temkin model in its linear form was adopted, the **Equation 7** was used.

$$q_e = B_1 ln(K_T) + B_1 ln(C_e) \quad \textbf{(7)}$$

The isotherm constants B_1 and K_T can be determined from the slope and the intercept of **Equation 7**, respectively. K_T is the equilibrium binding constant ($L \times mol^{-1}$) corresponding to the maximum binding energy and B_1 is related to the heat of adsorption. In this case, if the model well fit the experimental data it indicates that the heat of adsorption during the adsorption process linearly decreases with the coverage due to adsorbent–adsorbate interactions. The adsorption is characterized by a uniform distribution of binding energies.

Thermodynamic studies. Free energy ($\Delta G°$), entropy ($\Delta S°$), and enthalpy ($\Delta H°$) were determined (Chen et al. 2016, Fierro et al, 2018) for the TC adsorption on CH/OP (or CH/OP/TiO_2) at the three selected temperatures, 298, 288 and 278 K. In particular, the change in free energy ($\Delta G°$) was estimated from **Equation 8**:

$$\Delta G^\circ = - RT \, Ln \, K_{eq} \quad \textbf{(8)}$$

in which R is the universal gas constant (8.314 J/mol K), T is the temperature (K) and K_{eq} represents the equilibrium constant. So, the values of ΔH° and ΔS° were inferred combining **Equation 8** with **Equation 9** obtaining **Equation 10**.

$$\Delta G^\circ = \Delta H^\circ - T\Delta S^\circ \quad \textbf{(9)}$$

$$ln \, K_{eq} = - \frac{\Delta H^\circ}{RT} + \frac{\Delta S^\circ}{R} \quad \textbf{(10)}$$

Photodegradation of TC. The photodegradation of TC was accomplished, after its removal from water, by using UV, H_2O_2 and their synergic use also in presence of Fe^{2+} under Fenton conditions. A UV lamp was used to irradiate the adsorbent (UV fluorescent lamp, Spectroline, Model CNF 280C/FE, λ 254 nm, light flux 0.2 mW/cm^2; USA) adopting several contact times. Solid state photodegradation experiments, thus directly on the TC adsorbed were tried to attempt, and for this purpose the TiO_2 was added inside chitosan hydrogel to induce the formation of CH/OP/TiO_2.

RESULTS AND DISCUSSION

The proposed adsorbents were preliminary investigated from the morphological point of view, through macroscopic and microscopic analyses (**Figures S1, S2**).

The camera pictures reported in **Figures S1A-C** show the macroscopic view of the proposed single adsorbents. In particular**, Figure S1A** reports as chitosan film appeared without further modification, on the other hand **Figures S1B** and **C** show OP in powder and blended inside chitosan film (CH/OP), respectively. The microscopic observation (**Figures S1D, E**) of the CH/OP composite film, from two images related to different region of the same adsorbent indicated the heterogeneity of our sample, better evidenced in **Figure S2**, that reports the SEM image of OP occurring with irregular structures and cavities on the external surface, important key features for the adsorption of pollutants (Dai et al, 2019). For gaining insights into the surface chemical composition of the composite films prepared in this work, X-ray map images were acquired. As expected by chitosan films, and by main components of pomace (see ESI), i.e. cellulose, hemicelluloses, lignin, amino acids and/or proteins, the main presence of uniform distributed nitrogen and oxygen atoms was observed (**Figures S1F-G**). The finding was interesting for the proposed use of OP because, as reported recently by Dai et al. (2019), the surface oxygen functional groups could have important influence on the chemical properties of the adsorbents and thus in their ability in sequester pollutants, *i.e.* TC, from water. When the adsorbent CH/OP was enriched with TiO_2, the catalyst appeared uniformly distributed, as confirmed by results relative to the different film regions investigated (**Figures S1F-G**).

Adsorption of TC from water by OP and hybrid CH/OP adsorbents

In agreement with literature (Abdulghani et al.,2013; Abdel-Ghani et al.,2016) TC showed a characteristic UV-Vis absorption spectrum with two main absorption bands in the UV region, corresponding to $\pi \rightarrow \pi^*$ transitions. During this work, these bands were diagnostic for spectrophotometrically following the TC removal from water by using the proposed adsorbents. So, the OP was used both in powder and blended inside

chitosan films, for avoiding its potential dispersion in water as secondary pollutant. Chitosan represented only a physical support for OP, because, TC occurred not adsorbed by chitosan (*data not shown*). Starting from OP powder, fixing the TC concentration at 2.50×10^{-5}M, interesting results were obtained when the amount of the adsorbent was ≥25mg (**Figure 1A**). By choosing 1h as contact time, the adsorbed TC percentage increased by increasing the OP amount from 0.25 mg to 100 mg. At 100 mg of OP, about the 75% of the TC was removed, and, by elapsing the contact time, the adsorption was almost complete. On the other hand, when the OP amount was set at 25mg, while changing the TC amount (**Figure 1B**), results indicated as by diluting the TC solution, the adsorbed TC percentage increased. The same results were obtained when OP was blended with chitosan forming CH/OP (**Figures 1 C, D**). More specifically, different CH/OP films with different weights were used and indicated by numbering consecutively as CH/OP1, CH/OP2, CH/OP3 and CH/OP4 at the increasing of weight. According to results obtained for OP, the adsorption percentage increased at increasing the adsorbent weight (**Figure 1C**), maintaining constant, in this case, the contact time at 2h. Indeed, from CH/OP1 to CH/OP4, the removed TC percentage increased from about 25% to 75%. Once again, by diluting the TC solution, using the previous experimental condition and the CH/OP3 sample, the percentage of the TC removal from water increased (**Figure 1D**). Overall, this finding suggested that increasing the adsorbent weight and diluting the TC solution more free sites were available on the adsorbents (Rizzi et al., 2018b, Rizzi et al., 2019) for hosting TC evidencing the importance of the active site holding TC.

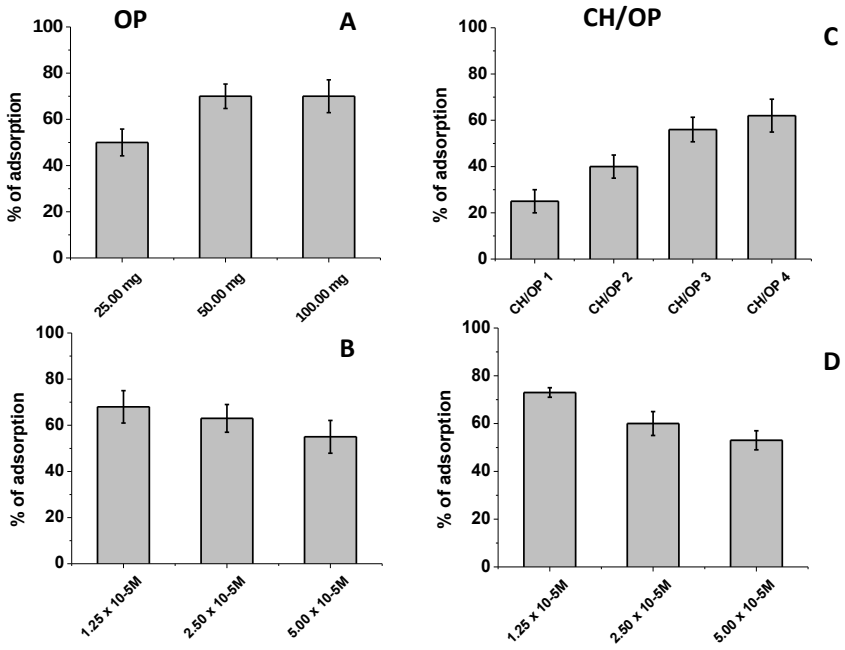

Figure 1: TC adsorption % ([TC]=2.50×10^{-5}M at pH 6) onto OP (**A**) and CH/OP (**C**) at different amounts and *viceversa* (**B, D**).

However, as arise from the contact time length and from the weights of the used films, the CH/OP composite material showed a lower adsorption efficiency, if compared with OP due to the presence of chitosan that retarded, as a whole, the process. To get more details about the adsorption process and to evidence the adsorption capacities of both the adsorbents, the q_t values were calculated (**Equation 1**) and compared, checking the best kinetic model able to fit the experimental data. **Figures 2A** and **B** show the q_t values for OP (**Figure 2A**) and CH/OP (**Figure 2B**), respectively, changing the adsorbent amounts. Interestingly, the q_t evolution of CH/OP tended to become linear if compared with results arisen from the use of OP. More specifically, the initial rapid TC adsorption observed for OP (**Figure 2A**) indicated as, at the beginning, the presence of

a large quantity of free sites on the surface of the adsorbents enhancing the process (Rizzi et al. 2019).

Moreover, this was because at the initial stage of adsorption the mass concentration of TC in the solution was high. (Dai et al, 2019). Elapsing the contact time, the plateau region was reached, and this finding could be due to the repulsive force effect between TC molecules in solution and those adsorbed on the adsorbent, together with the reduced number of free active sites, that as a whole retarded the adsorption process (Chen et al.,2016). When the CH/OP was considered (**Figure 2B**), the initial rapid change of the q_t values was absent. Since chitosan films without OP are unable in adsorbing the TC, the results indicated that the presence of the linear polysaccharide limited the TC uptake, overall retarding its removal from water. However, also in this case, the q_t values tend to level off, with elapsing the contact time. Further, when blocked inside CH, the OP was present as aggregates and not as fine powder contributing in reducing the adsorbent surface area. It is noteworthy that for both the adsorbents, by increasing their amount, the relative adsorption of TC molecules increased (see the plateau region beginning that was quickly reached in presence of the largest amount of the adsorbent); on the other hand, the adsorption capacity decreased. This result, in agreement with literature (Rizzi et al., 2018b, Rizzi et al. 2019), can be explained considering that, using a large amount of adsorbent, the adsorption sites partially remained unsaturated during the adsorption process, reducing as a whole the q_t values, nonetheless the TC removal was quite complete.

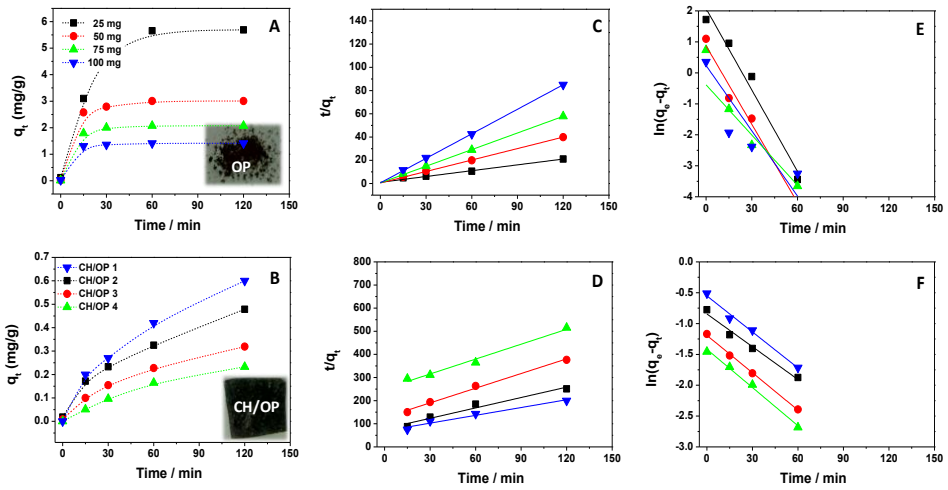

Figure 2: Effect of OP (**A**) and CH/OP (**B**) amounts on the q_t values during the TC adsorption (2.50×10^{-5}M at pH 6); Pseudo-second (**C, D**) and pseudo-first order (**E, F**) kinetic models related to OP and CH/OP, respectively.

The kinetic models well agree with these findings. In particular, by using the q_t values reported in **Figures 2A** and **B,** the results reported in **Figures 2C-F**, applying the pseudo-first (**Equations 2)** and pseudo-second (**Equations 3)** order kinetic models, were obtained. The calculated R^2 values and the correspondence between the adsorption capacity at equilibrium, $q_{e,cal}$, (calculated from the kinetic elaboration) and $q_{e,exp}$ (experimentally inferred form **Figures 2A** and **B**) indicated that the TC adsorption on OP followed a pseudo-second order kinetic ($R^2 > 0.99$), while on CH/OP, a pseudo-first order one ($R^2 > 0.99$). Both for OP in powder and CH/OP the kinetic constants are reported in **Table S1**. The pseudo second-order kinetic model showed that the adsorption process was a combination of physical and chemical adsorption, and as suggested by Dai et al (2019) the adsorption mechanism of TC on OP should be mainly due to chemical adsorption. Indeed, under this condition, the adsorption equilibrium should be rapidly reached, and this was consistent with the experimentally observed adsorption equilibrium with a shorter time. On the other hand, when CH/OP was taken

into account the role of other factors should be considered more important and the diffusion of TC inside the adsorbent could play a key role due to the presence of chitosan that hindered the TC adsorption. To gain more insights into the delayed of the TC adsorption process on CH/OP, the TC concentration was changed observing changes during the adsorption on the CH/OP film: whereas the adsorption efficiency decreased at increasing the TC amount (**Figures 3A**), the adsorption capacities of the adsorbent (q_e) increased from 0.1 to 0.5 mg/g. The high TC concentration induced a greater mass transfer, increasing the adsorption capacity indicating the important role of diffusion. So, the Weber equation $q_t=K_i t^{1/2}$ was applied, by varying the amount of TC, and a liner trend was observed (**Figure 3B**). The kinetic constants related to the intra-domain diffusion rate in mg/(g×min$^{0.5}$) were calculated. Increasing the TC concentration, the following K_i values were obtained: 0.02mg/(g×min$^{0.5}$), 0.03mg/(g×min$^{0.5}$) and 0.07mg/(g×min$^{0.5}$). So, when CH/OP adsorbent was used, the intra-domain diffusion could be considered the main mechanism controlling the sorption process (Moussavi and Khosravi,2011).

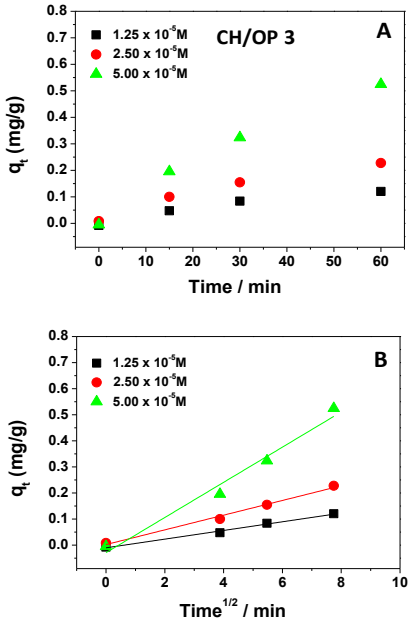

Figure 3: Effect of TC amount, when CH/OP 3 is used, on the q_t values (**A**), Weber-Morris plot using CH/OP 3 changing the amount of TC (**B**).

More information were obtained by studying the TC adsorption influence on the CH/OP film swelling (**Figure S2**). The swelling ability (**Equation 4**) of chitosan films in water is well-known (Becerra et al.,2017; Thomas and Alghamdi,2018; Rizzi et al.,2018). In our case, the CH/OP film increased its weight of more 300% when swollen in water, while, in presence of TC, the swelling was about 200%. This could indicate a more hydrophobic character of the composite adsorbent when the TC was adsorbed. This result suggested the existence of weak electrostatic interactions between TC and OP, probably through the chitosan amino groups, main responsible of the chitosan film swelling behavior properties (Rizzi et al.,2016a). For that reason, the effects of pH and ionic strength on the TC adsorption on the propose adsorbents were explored. It noteworthy that the same experiments about the adsorption of TC were performed carefully investigating also CH/OP/TiO_2, as adsorbent material. The results suggested that the TiO_2 addition did not affect the adsorption process characteristics.

Salts and pH effects on TC adsorption. The molecular structure of TC (**Figure 4A**) has three dissociation constants (Dong et al. 2018). At pH < 3.3 (pKa_1), TC exists in the cationic form (TCH_3^+), in the range of 3.3–7.7 (pKa_2), the main form is the zwitterion ($TCH_2^{\pm}$), and at pH > 7.7 is in the two anionic forms, TCH^- and TC^{2-}(the latter for pH > pKa_3 9.7) (Chen et al, 2016). So, the TC adsorption onto pomace was investigated at several pH values. More specifically, a small amount of pomace was used, *i.e.* 25 mg, fixing the contact time at 1h. The percentages of TC adsorption were evaluated and reported in **Figure 4B**. Interestingly, a very low TC adsorption was observed at pH 2. On the other hand, above neutral condition of work, the TC adsorption increased. On this base, the pH_{PZC} of the adsorbent was experimentally inferred (**Figure 4C)** using the

drift method (Rizzi et al. 2018b) and a pH_{PZC} around pH 8 was obtained. The results indicated that the adsorbent was positively and negatively charged below and above this pH value, respectively. So, at pH < 4, the observed low adsorption capacity suggested repulsive forces between TCH_3^+ and the positively charged surface of the adsorbent, because the electrostatic interactions predominated. However, the competition between the H^+ ions and the cationic TCH_3^+ for binding sites on the OP surface cannot be ruled out (Fan et al. 2016). On the other hand, the incrementing TC adsorption observed in the pH range 7-10 (**Figure 4B**), exactly near the pKa_3 of TC, indicated the presence of a good interaction between $TCH_2^{\pm}$, TCH^- and the neutral surface adsorbent. At the pH > 10, being mainly present the TC dianionic form (TC^{2-}), there is again a slight electrostatic repulsion with the negatively charged surface of OP, determining the slight reduction of the antibiotic adsorption. These observations could be explained considering that, in the range of solution pH 7-10, the prevailing zwitterionic form of the TC promoted the adsorption by interactions not only of electrostatic nature, but also through hydrogen bonding, involving mainly oxygen groups of TC and OP (Dai et al, 2019), electron-donor acceptor and π–π stacking between the antibiotic aromatic rings and the OP surface.

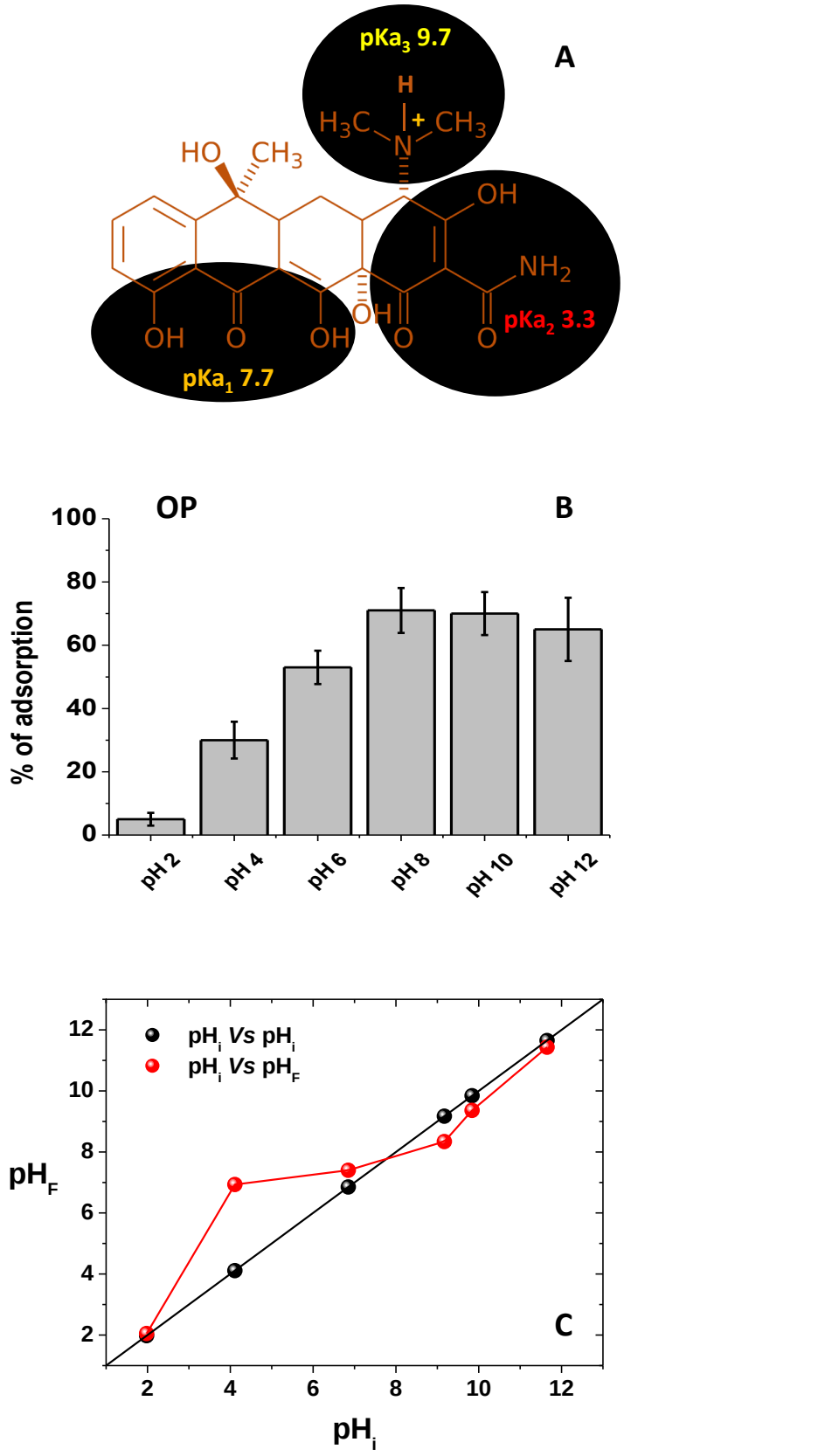

Figure 4: Molecular structure of TC evidencing its pK_a values **(A)** % of TC adsorption (from TC solution 2.50×10^{-5}M) on OP (25 mg) at different pH values (**B**) and the drift plot used to infer the pH_{PZC} of the OP (**C**)

The presence of electrostatic forces was confirmed by performing adsorption experiments in presence of different salts NaCl, NaI, KCl, LiCl, $MgCl_2$, $CaCl_2$ (0.1M), using 25mg of pomace, at pH 6, and 1h as contact time (**Figures S3**). The use of salts containing bivalent ions, as Ca^{2+} and Mg^{2+} (**Figure S3A**), more affected the adsorption process decreasing significantly the TC removal from water. Results agree with the presence of electrostatic forces between TC and OP. Given the pH_{PZC} value were 8 the surface OP was expected to be positively charged at the pH value 6. So, Cl^- should be preferentially adsorbed onto CH/OP by electrostatic interaction. Dai et al, (2019) suggested that the salt could occupy sites on the adsorbent, and due to the surface heterogeneity, competitive adsorption of TC and salts should be considered, decreasing the adsorption capacity in TC. (Dai et al, 2019)

Since the behavior exhibited by NaCl, NaI, KCl and LiCl was the same, NaCl was selected among them for studying the monovalent electrolyte concentration effect, by increasing its concentration from 0.1M to 2M. Moreover, also the bivalent cation concentration was increased, choosing Mg^{2+}-based salts, $MgCl_2$ and $MgSO_4$, due to the $CaCl_2$ lower water solubility (**Figure S3B**). However, independently by the counter-ion Cl^- or SO_4^{2-}, in presence of high Mg^{2+} amounts, the TC adsorption failed, indicating the main role of the cation Mg^{2+}. In this case, the salt not only should affect Columbian forces but also Mg^{2+} inhibited the TC adsorption due the coordination of the TC ketoenolate moiety as well documented in literature forming the TC-Mg^{2+} complexes (Palm et al.,2008). Results confirmed the presence of electrostaic interaction and the role of the TC ketoenolate moiety involved trough the formation of H-bonding between TC and the main component of OP as supposed by Dai et al, (2019) in a similar system.

Release of TC: reuse of OP and CH/OP. Although, different organic solvents were tentatively used, only solutions having high ionic strength allowed the TC release from

the adsorbents. Not surprisingly, the presence of salts in solution more affected the removal of TC favoring, after the TC adsorption, its desorption. The screening of different salts was performed at concentrations of 0.2 and 2M (except for $CaCl_2$ used only at 0.2M due to its lower solubility) (**Figure 5A**), adopting 1h as contact time. Regarding to OP, bivalent cations as expected favored the release: i.e. $MgCl_2$ 0.2 M induced about the 90% of the TC desorption against the 40 % obtained in presence of $CaCl_2$. The coordination of Mg^{2+} and TC was proposed. On the other hand, the slight TC release was observed by using salts containing monovalent cations also increasing the salt concentration to 2M. In this case LiCl favored the TC release if compared with NaCl or Na_2SO_4. Selecting $MgCl_2$, when CH/OP was used, 24h were needed to obtain the same result; however, the concentration of salt was increased to 2M (**Figure 5B**), strengthening the differences between OP and CH/OP. For evidencing the key role of the $MgCl_2$, the $MgSO_4$, so changing the counter ion, was used in presence of CH/OP showing that, after 24h, only the 50% of the adsorbed TC was recovered. In details, in **Table S2**, the % of TC desorption are reported at several contact time. Results indicated also the possible role of Cl^-, with respect SO_4^{2-}, that replaced the TC molecules favoring its release in solution. Probably in this case, due to the small size of Cl^- if compared with SO_4^{2-}, it diffused easer trough CH/OP favoring the TC recover.

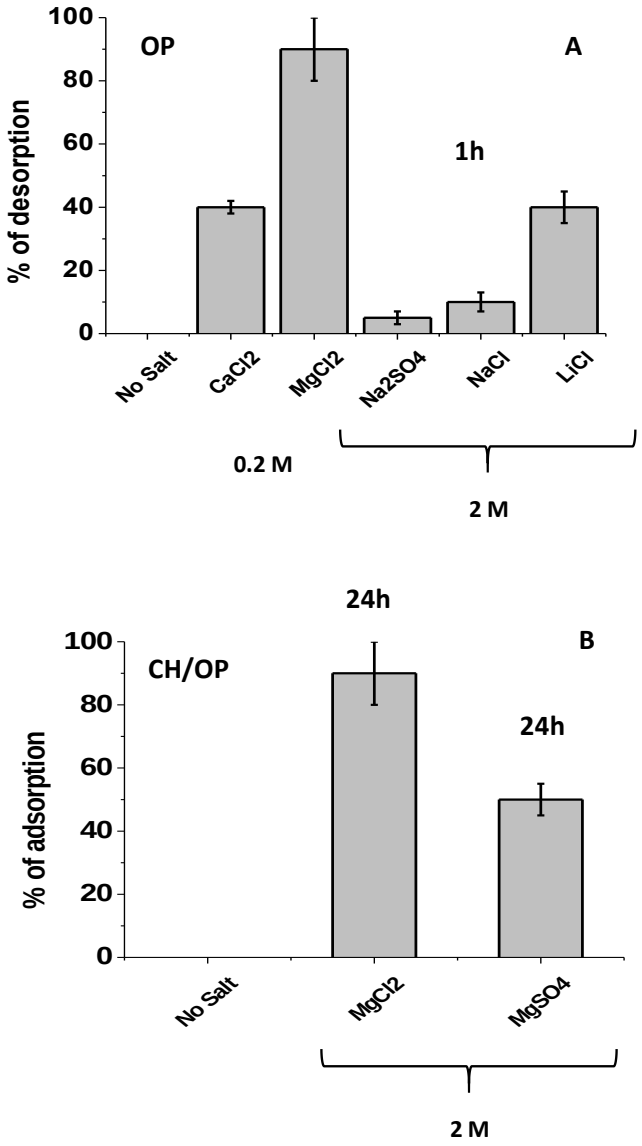

Figure 5: % of TC desorption from OP (**A**) and CH/OP 3 (**B**) in presence of salts: the time need for the desorption is indicated; the adsorption was performed by using 100 mg of OP and CH/OP 3 swelled in a TC solution (2.50×10^{-5}M at pH 6) for 1 h and 2h respectively.

Notwithstanding the less efficiency in comparison with OP, the CH/OP composite film appeared to be the best candidate for a real wastewater treatment due to the manageability of chitosan film with respect OP powder; so it was subjected to adsorption consecutive experiments, with the aim of evaluating its loading capacity. CH/OP was put in contact with a TC solution (2.50×10^{-5}M), and, after its cleaning, that solution was substituted with a fresh one. UV-Vis spectra were acquired at appropriate

contact times for evaluating the percentage of the adsorbed TC (**Table S3**). So, under our experimental conditions, the CH/OP film was very performant for the TC removal from water, also after 8 consecutive cycles of adsorption. These results emphasized the use of this ecofriendly and low-cost approach for wastewater treatments (Fresner, 1998), even though the contact time, necessary to obtain efficiencies of adsorption greater than 50%, raised from 7h to 64h, at increasing the adsorption cycles number. The release of the total amount of the adsorbed TC was also attempted, obtaining a release of 95%. Moreover, the ability to adsorb and desorb the pollutant for several consecutive cycles of adsorption and desorption was investigated. CH/OP was dipped in the TC solution (2.50×10^{-5}M); then, after 2 h (this time could be also increased for increasing the TC adsorption), the film was removed from the TC solution and dipped again in a 2M $MgCl_2$ solution for other 2h, obtaining the TC release (**Table S4**). Three cycles of adsorption/desorption were accomplished, and, after each cycle, the film was washed with fresh water for removing the electrolyte excess, that otherwise could slow down the subsequent TC adsorption. After three cycles, the very good performance of the CH/OP composite is evident (**Table S4**), suggesting that more than 3 cycles could be performed.

Isotherm of adsorption. A comprehensive investigation using the Langmuir, Temkin and Freundlich models (**Equations 5-7**) was performed on CH/OP (**Figures 6** and **Table 1**). Since the obtained R^2 values, the adopted models well described the experimental data, confirming the heterogeneous surface of the adsorbent. The favorable character of the adsorption process was also evidenced by the n values arisen from the Freundlich equation. Indeed, *n* values >1, in the range 1.45-1.53, were obtained during this study by changing the temperature values. Overall, the isotherm

parameters are reported in **Table 1** at different temperatures evidencing the role of the latter as arise from the thermodynamic analysis.

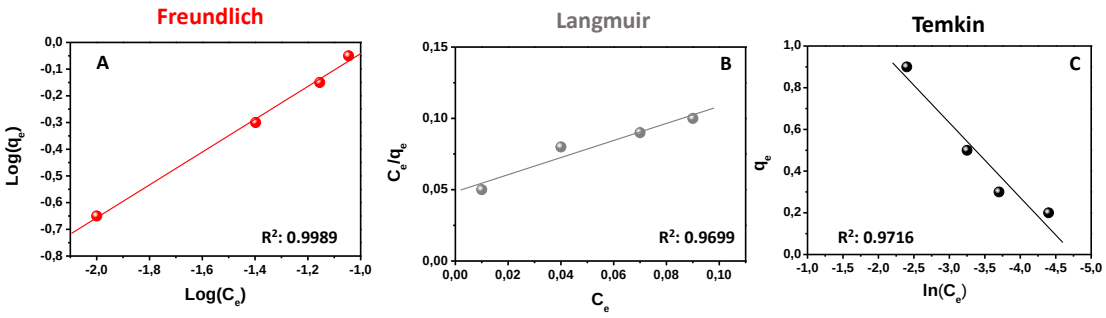

Figure 4: Isotherms of adsorption when CH/OP 3 is used.

	Freundlich isotherm model			Langumir isotherm model			Temkin isotherm model		
T 298 K	K_F (L×mg^{-1})	n	R^2	K_L (L×mg^{-1})	Q_0 (mg×g^{-1})	R^2	K_T(L×mol^{-1})	B_1	R^2
	4.20	1.53	0.9989	15.38	1.60	0.9699	207.12	0.30	0.9716
	Freundlich isotherm model			Langumir isotherm model			Temkin isotherm model		
T 288 K	K_F (L×mg^{-1})	n	R^2	K_L (L×mg^{-1})	Q_0 (mg×g^{-1})	R^2	K_T(L×mol^{-1})	B_1	R^2
	4.00	1.50	0.9991	14.85	1.55	0.9685	204.50	0.31	0.9753
	Freundlich isotherm model			Langumir isotherm model			Temkin isotherm model		
T 278 K	K_F (L×mg^{-1})	n	R^2	K_L (L×mg^{-1})	Q_0 (mg×g^{-1})	R^2	K_T(L×mol^{-1})	B_1	R^2
	3.85	1.45	0.9989	14.60	1.46	0.9710	201	0.28	0.9765

Table 1: Isotherm parameters for the adsorption of TC onto CH/OP3

Thermodynamic analysis for CH/OP. Three temperature values were adopted, i.e. 278, 288 and 298 K by using CH/OP 3 and TC solution with a concentration of 2.5 × 10^{-5} M. At first glance the results reported in **Figure 6A**, indicated as increasing the

temperature values increasing the percentage of TC adsorption from water. At 298 K, after 6h adopted as contact time the removal was almost complete. The endothermic character was easily inferred. In order to find the thermodynamic parameters, the K_{eq} values were calculated at each temperature (**Table S5**) and by using **Equations 8, 9**, the ΔG° values were inferred. Subsequently, by using **Equation 10**, ΔH° and ΔS° were obtained (**Table S5**) plotting ln (K_{eq}) versus 1/T (**Figure 6B**). The process occurred with a $\Delta G°_{298K}$=-13.20KJ/mol and ΔH°=+50.00KJ/mol indicating the spontaneous and endothermic character of the process, respectively. The positive value of ΔS°=+210 J/mol K suggested as the randomness at the surface of the adsorbent increased. (Dai et al, 2019)

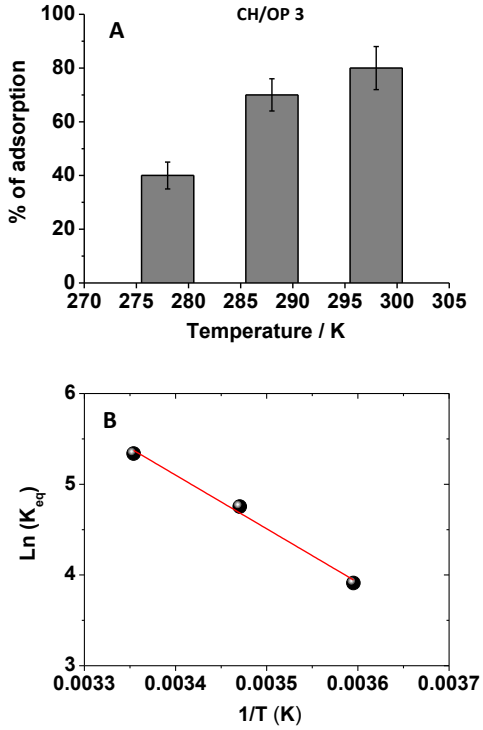

Figure 6: % of TC adsorbed at different temperature values (**A**); ln (K_{eq}) *vs* 1/T. In particular, the K_{eq} represent the equilibrium constant at the selected temperature value (298K, 288K and 278K) (**B**). CH/OP 3 is used as adsorbent.

Degradation of TC free in solution after the desorption from CH/OP.

It is worth to mention that the photodegradation of TC is well known since several years and interesting information are reported in litearture (Jiang et al.,2018, López-Peñalver et al., 2010). In order to show as the adsorbed TC can be also photodegraded, as first step, CH/OP/TiO_2 was used. After the adsorption of TC, the adsorbent was irradiated with a UV lamp adopting different contact time, 1, 2, 4 and 8h. Further, the experiments were performed with wet (15 mL or 30 mL of water) and dried CH/OP/TiO_2. In all of examined conditions of work, the adsorbed TC was poorly and very slowly degraded, also extending the contact time. The slight degradation, nonetheless the presence of TiO_2, was attributed to the presence of phenols from the pomace, whose antioxidant activity along with their high absorbance in the UV-Vis region is well-known and able to inhibit the TC degradation.

For example, in **Figure 7A,** the UV-Vis spectrum of the phenols purposely desorbed by the used pomace is reported, highlighting the absorption band of the antioxidants at λ<300 nm screening the UV radiation. In order to overpass this problem, the irradiation with UV light was attempted by swelling the adsorbents loaded with TC in a $MgCl_2$ solution (2M). Under this condition, the release of TC should increase its photodegradation. However, by comparing the results obtained from CH/OP and CH/OP/TiO_2, it was observed how the use of only UV light was enough for photodegrading the outcoming TC. The synergic action of TiO_2 and UV did not happen. Indeed, after 4h of irradiation time, about the 70% of the adsorbed TC was destroyed in both cases. As a result, the photodegradation was performed after the release of TC from CH/OP avoiding, at moment, the use of the CH/OP/TiO_2 adsorbent.

In a subsequent experiment, the TiO_2 was added as suspension in the solution containing the released TC. More specifically, CH/OP 3 was swollen in a TC solution with a concentration of 2.5×10^{-5}M, and after the almost complete removal of the TC,

the release in $MgCl_2$ was performed. As seen in **Figure 7B**, a very low TC degradation was observed if the TC solution was irradiated with UV (λ=254 nm) light in absence of TiO_2, indicating that the TC molecule was photochemically resistant. Indeed, 6h were necessary to degrade about the 80 % of the pollutant (condition 1, in **Figure 7B**).

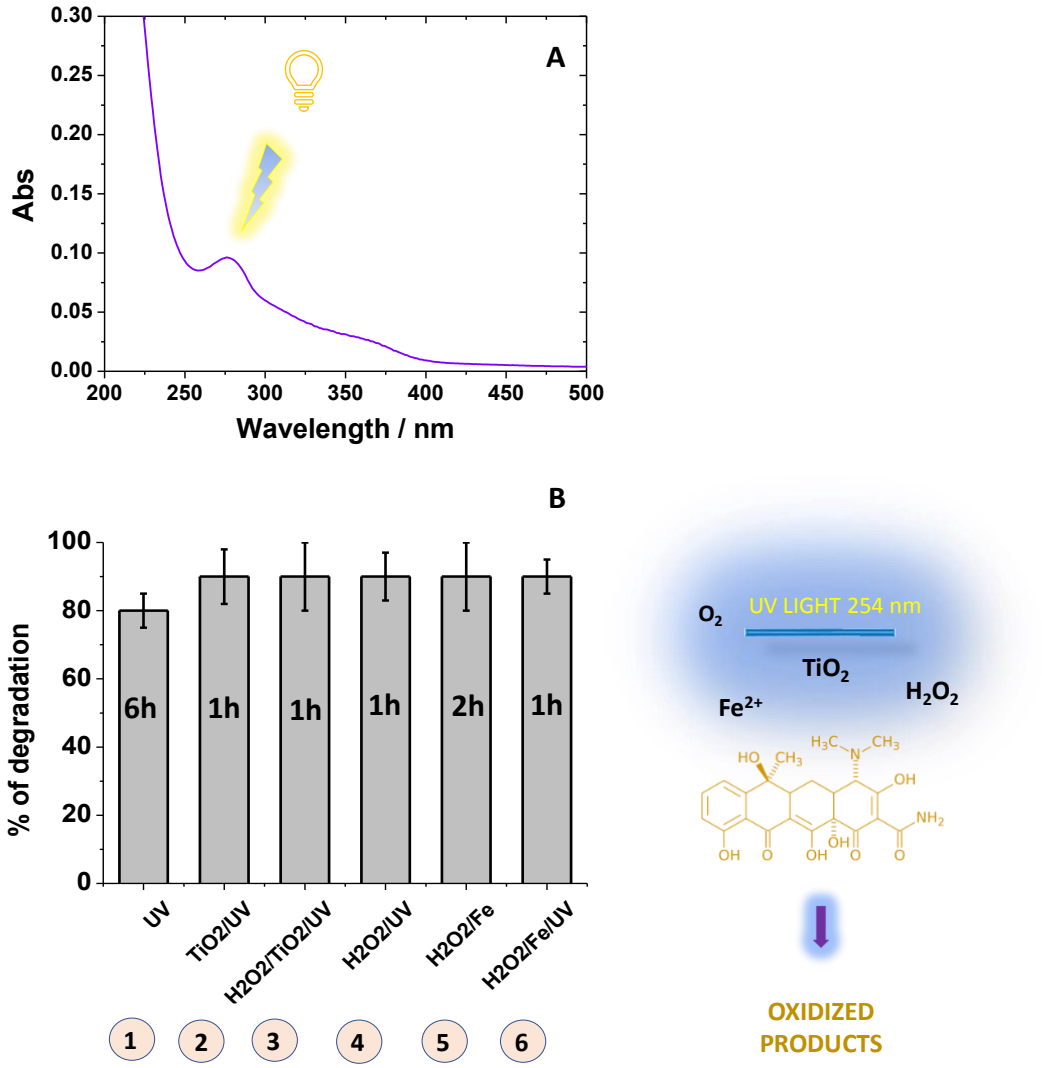

Figure 7. UV-Vis spectrum of phenols from OP **(A);** Degradation of 15 mL of a TC solution (2.50×10^{-5} M) under different experimental conditions: **(1)** irradiated with UV light; **(2)** 1mg of TiO_2 suspended in the TC solution and irradiated with UV light; **(3):** 1mg of TiO_2 suspended in the TC solution in presence of 1mM H_2O_2 and irradiated with UV light; **(4)** TC solution in presence of H_2O_2 1mM and irradiated with UV light; **(5)** TC solution in presence of H_2O_2 1mM and Fe^{2+} 1.0×10^{-5}M; **(6)** TC solution in presence of H_2O_2 1mM and Fe^{2+} 1.00×10^{-5} M irradiated with UV light (**B**)

This finding could be attributed to a small amount of •OH formed in the bulk solution under these conditions. On the other hand, in presence of the TiO_2 as photocatalyst,

purposely added in the solution, the degradation and inactivation of TC was observed under our experimental conditions within 1h (condition 2 in **Figure 7B**). In the presence of TiO_2, the production of active species such as •OH, hole and superoxide ions make the process very efficient (Vega and Valdes, 2018). The addition of H_2O_2 to TiO_2 suspensions improved (Safari et al. 2015) the process obtaining the 100 % of TC degradation in short time, practically the process occurred accomplished after 1h (condition 3). As previously explained, additional •OH are produced under this condition. Indeed, the synergistic use of UV/H_2O_2, H_2O_2/O_3, Fenton, electro-Fenton, and photo-Fenton showed a good performance for the removal of TC from an aquatic environment. Exploring various combination of UV light, H_2O_2 and Fe as photodegrading agents, as reported in **Figure 7B** (condition 4), when the system H_2O_2/UV was considered, the greater degradation of TC was completed in 1h. By comparing this experimental condition with the use of the only UV light that required ~6h for 80 % of the TC degradation, it was clear that the UV/H_2O_2 treatment was more effective in the degradation of TC. If the Fenton process was considered (**Figure 7B**, condition 5), the degradation occurred slightly retarded (in 2h), but by adding the UV irradiation, the time necessary for a complete degradation was halved (**Figure 7B**, condition 6). The production of hydroxyl radicals that occurred during the decomposition of H_2O_2 in the presence of ferrous ions, increased in presence of UV–Vis irradiation, thanks to the regeneration of ferrous ions, thus forming additional •OH as reported in the following scheme (Rossi Bautitz and Nogueira., 2007):

$$Fe^{2+} + H_2O_2 \rightarrow Fe^{3+} + OH^- + \bullet OH$$

$$Fe^{3+} + H_2O + h\nu \rightarrow Fe^{2+} + \bullet OH + H^+$$

Overall, during this work different method for photodegrading the TC were presented in order to demonstrate as the antibiotic adsorption process on CH/OP and/or OP could be considered a very fashionable approach to treat wastewater, recovering and/or photodegrading TC.

3.8 *In flux* experiments. When in flux experiments were performed, the CH/OP was firstly swollen inside a syringe-like column (3.00×5.00 cm) with fresh water. A peristaltic pump, working at 3.00 mL/min, was used to make a 2.50×10^{-5}M TC solution (15mL) flow through the adsorbent (**Figure 8**). The TC flow through the column was accomplished, and the eluting water was collected and spectrophotometrically investigated. After 1h, the TC adsorption of ~50% was observed, showing that the presented material can be also used for *in flux* experiments. The TC desorption was also obtained by using a $MgCl_2$ solution.

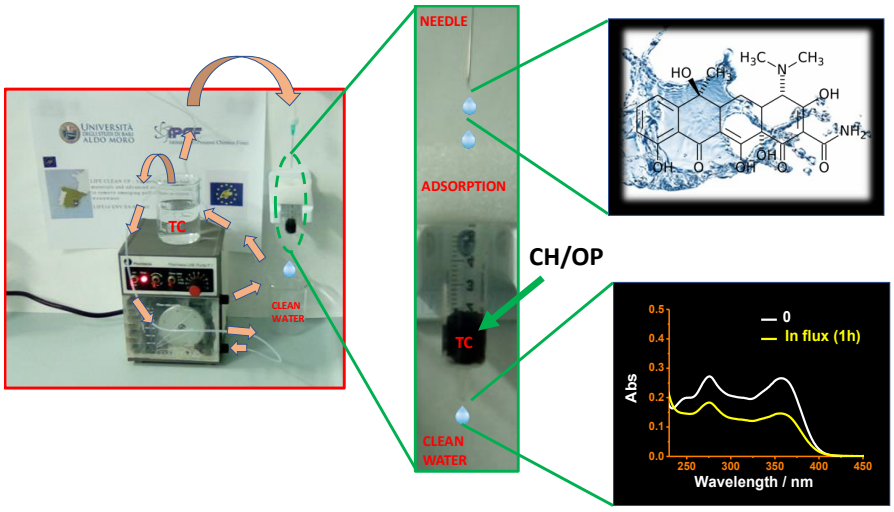

Figure 8: Camera picture of the experimental setup adopted during the *in flux* experiments using CH/OP 3 as adsorbent and TC as model EP. The arrows in the Figure indicate the direction of the flux

Comparison of Q_{max} values obtained in literature for removal of TC from water by using different adsorbent materials.

Table 2 reports the comparison of Q_{max} values (the maximum adsorption capacity) of the studied adsorbents. Many papers are reported in literature about the TC removal and for this purpose the most representative have been selected, from 2012 to nowadays, proposing the comparison of different typology of adsorbents. It is worth to mention that in the most cases, different temperature and pH values, and conditions of work, were adopted. Results indicated that very high adsorption capacities were obtained, as for composite cryogel, KOH-activated carbon or active carbon from tomato, if compared with our results. The use of sulfonated tea waste and ground spent coffee, as more greener production approaches, occurred more interesting for our aim; however, if the production of the former required very hard conditions of work (Authors reported the use of high temperature and H_2SO_4 for 4h), on the other hand the latter adsorbent was held in a thermostatic chamber at 60 °C for 48 h. So, beside the high adsorption capacities under optimized condition of work, all of listed adsorbents required pre-treatment (increasing the associated costs) if compared with our work, or in same case hard acid condition of work far for cleaner and sustainable production technologies. On the other hand, a greener approach is presented, for the first time, in this paper avoiding the use of additional treatments and hard condition of work proposing agricultural wastes as olive pomace as resources. Indeed, in the work of Dai et al. (2019) the use of ground spent coffee did not investigated the possibility to recover the pollutant or perform consecutive cycles of adsorption and/or desorption. So, all of the adsorbents

reported in **Table 2** could be considered secondary pollutant and should be removed from the environment. On the other hand, with our work, the olive wastes are removed from the environment and used to clean water from pollutants. The latter is recovered proposing safe ecofriendly adsorbents, and as alternative the TC can be photodegraded far from water after the recover avoiding the production of more toxic metabolites in water. So, nonetheless, during this study the obtained Q_{max}, arisen from the Langmuir isotherm, are lower than values reported for other materials, several consecutive cycle of adsorptions (or adsorption/desorption) are proposed increasing the adsorption capacities showing other advantages, as the reuse of safe adsorbents, overpassing this drawback. Overall, avoiding the use of chitosan, the Q_{max} could be increased to16 $mg \times g^{-1}$ and to much more greater values considering the adsorption/desorption approaches. Furthermore, the proposed adsorbents exhibit another advantage as described in the following: they are able to remove other pollutants, and their mixture, presenting an adsorbent for wide ranging applications useful for industrial applications.

ADSORBENT	Q_{max} (mg×g^{-1})	References
$MnFe_2O_4$/activated carbon	283[a]	Shao et al., 2012
graphene oxide	313,5	Gao et al., 2012
Rice husk ash	4	Liu et al., 2012
Porous carbon from waste hydrochar	25	Zhu et al., 2014
Pumice stone	20,02	Guler et al., 2014
Amino-Fe (III) functionalized SBA15	46 [a]	Zhang et al., 2015
Activated carbon prepared from tomato	416,7	Sayğılı et al., 2016
Graphene oxide/calcium alginate composite fibers	312,5	Fan et al., 2016
KOH-activated graphene	532,6	Ma et al., 2017
Composite cryogel	2042	Yeşilova et al., 2018
Oxidized activated carbon	634	Qin et al, 2018
Sulfonated tea waste	381	Ahsan et al, 2018
spent coffee ground	64.89 123.46	Dai et al, 2019
Zeolitic imidazolate frameworks	446.9	Dehghan et al, 2019
Chitosan/olive pomace film	1,60 (x cycle)	This study
Olive pomace	16 (x cycle)	This study

a: these values have been adopted by literature and transformed in mg/g

Table 2: Comparison of Q_{max} values obtained in literature for removal of TC from water by using different adsorbent materials.

Removal of Ketoprofen and Diclofenac and their mixture in presence of TC. The use of the same chitosan-based adsorbent (CH/OP) was proposed also for the removal of other EPs, such as ketoprofen and diclofenac from water (**Figure S5,** see the discussion in ESI). Indeed, the removal of these emerging pollutants is also an actual concern (De Franco et al.,2018; Jankunaite et al.,2017). The very good performances showed by this composite material suggests of proposing the CH/OP film for the

removal of different class of EPs. Therefore, an EPs mixture, also in presence of TC, was studied, demonstrating as the TC adsorption was not affected by the presence of other pollutants. In particular, the mixture of ketoprofen, diclofenac and tetracycline was studied (ketoprofen: 2.5 mg/L, diclofenac, 3.0 mg/L and TC: 5.0 mg/L) in presence of CH/OP 3 by monitoring the UV-Vis spectrum. **Figures 8** shows the obtained results indicating as the removal of TC was obtained also in presence of other pollutants. Further, beside the adsorption of TC, the removal of other EPs occurred also in the mixture.

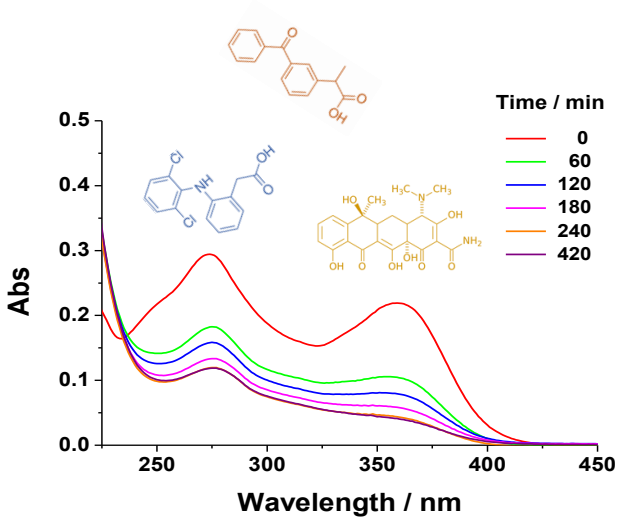

Figure 9: UV-Vis spectra of a mixture of emerging pollutants, ketoprofen, 2.5 mg/L, diclofenac, 3.0 mg/L and TC: 5.0 mg/L, acquired at different contact time if in presence of CH/OP 3.

CONCLUSIONS

During this work the first use of olive solid waste, olive pomace (OP), as adsorbent, to remove the antibiotic tetracycline (TC) from water is presented. More specifically, the OP was studied both in powder (as received) and blended inside a chitosan membrane. The latter acted as physical platform, for OP obtaining chitosan/OP (CH/OP) films, avoiding the dispersion of the waste in water as secondary pollutants. To photodegrade

the adsorbed TC, the use of TiO_2 is proposed mixing the photocatalyst inside the film (obtaining CH/OP/TiO_2). However, this approach occurred not useful and the TC photodegradation was obtained after its release in $MgCl_2$ from the adsorbent by using AOPs. Subsequently, the use of CH/OP was evaluated if the TC removal occurred in presence of EPs as ketoprofen and diclofenac showing as the adsorption of TC was not affected. Further, ketoprofen and diclofenac were also removed from water highlighting the high performance of CH/OP for environmentally friendly applications. A comprehensive investigation about the use of these adsorbents is therefore presented in the paper evaluating the adsorption capacities, the kinetic, the thermodynamic and the isotherms of the adsorption processes adopting TC as model pollutant. The possibility to use and re-use the adsorbent for consecutive cycles of adsorption is presented. Finally, preliminary *in flux* measurements were also tried to attempt indicating that a possible industrial scaling up could be achieved with the future perspective to modify the adsorbents to remove a largest class of pollutants.

ACKNOWLEDGEMENTS.

This work was supported by the LIFE+ European Project named **LIFE CLEAN UP** ("Validation of adsorbent materials and advanced oxidation techniques to remove emerging pollutants in treated wastewater" – LIFE 16 ENV/ES/000169).

REFERENCES

Abdel-Ghani, N.T., Rawash, E.S.A., El-Chaghaby, G.A., 2016. Equilibrium and kinetic study for the adsorption of p-nitrophenol from wastewater using olive cake based activated carbon. Global J. Environ. Sci. Manage. 2(1),11-18;

Abdulghani, A.J., Jasim, H.H., Hindawi, A.S.H., 2013. Determination of Tetracycline in Pharmaceutical Preparation by Molecular and Atomic Absorption Spectrophotometry and High Performance Liquid Chromatography via Complex Formation with Au(III) and Hg(II) Ions in Solutions. Int. J. Anal. Chem., http://dx.doi.org/10.1155/2013/305124

Ahmed, M.J., Hameed, B.H., 2018. Removal of emerging pharmaceutical contaminants by adsorption in a fixedbed column: A review. Ecotoxicol. Environ. Saf. 149,257–266;

Ahsan, A., Katla, S.K., Islam, T., Hernandez-Viezcas, J.A., Martinez, L.M., Díaz-Moreno C.A., Lopez, J., Singamaneni S.R., Banuelo, J., Gardea-Torresdey, J., Juan C. Noveron, J.C, 2018. Adsorptive removal of methylene blue, tetracycline and Cr (VI) from water using sulfonated. Environmental Technology & Innovation 11, 23–40

Becerra, J., Sudre, G., Royaud, I., Montserret, R., Verrier, B., Rochas, C., Delair, T., David, L., 2017. Tuning the Hydrophilic/Hydrophobic Balance to Control the Structure of Chitosan Films and Their Protein Release Behavior. AAPS PharmSciTech. 18,1070-1083;

Belayutham, S., Gonzalez, V.A., Yiu, T.W., 2016. A cleaner production-pollution prevention based framework for construction site induced water pollution, J. Clean. Prod. 135,1363-1378;

Chen, Y., Wang, F., Duan, L., Yang, H., Gao, J. 2016. Tetracycline adsorption onto rice husk ash, an agricultural waste: Its kinetic and thermodynamic studies. J. Mol. Liq. 222,487–494;

Dai, Y., Zhang,K., Meng,X., Li,J., Guan,X., Sun,Q., Sun,Y., Wang, W., Lin,M., Liu, M., Yang, S., Chen,Y., Gao, F., Zhang, X., Liu, Z. 2019. New use for spent coffee ground as an adsorbent for tetracycline removal in water. Chemosphere, 215, 163-172;

De Franco M.A.E., de Carvalho C.B., Bonetto M.M. , Soares R.P., Feris L.A. 2018. Diclofenac removal from water by adsorption using activated carbon in batch mode and fixed-bed column: Isotherms, thermodynamic study and breakthrough curves modeling. J. Clean. Prod.,181,145-154;

Dehghan,A., Zarei,A., Jaafari,J., Shams,M., Khaneghah, A.M. 2019. Tetracycline removal from aqueous solutions using zeolitic imidazolate frameworks with different morphologies: A mathematical modelling. Chemosphere, 217, 250-260;

Dong, H., Jiang, Z., Zhang, C., Deng, J., Hou,K., Cheng,Y., Zhang,L., Zeng, G.2018. Removal of tetracycline by Fe/Ni bimetallic nanoparticles in aqueous Solution. J. of Colloid and Interface Science 513, 117–125.

Fan H.T., Shi L.Q., Shen H., Chen X., Xie K.P. 2016. Equilibrium, isotherm, kinetic and thermodynamic studies for removal of tetracycline antibiotics by adsorption onto hazelnut shell derived activated carbons from aqueous media. RSC Adv.,6(111),109983-109991;

Gao, Y., Li, Y., Zhang, L., Huang, H., Hua, J., Shah, S.M., Su, X. 2012.Adsorption and removal of tetracycline antibiotics from aqueous solution by graphene oxide. J. Coll.and Int. Sci., 368, 540–546;

Gubitosa J., Rizzi V., Lopedota A., Fini P., Laurenzana A., Fibbi G., Fanelli F., Petrella A., Laquintana V., Denora N., Comparelli R., Cosma P. 2018. One pot environmental friendly synthesis of Gold Nanoparticles using *Punica Granatum* Juice: a novel antioxidant agent for future dermatological and cosmetic applications. J. Coll. Int. Sci.521,50-61;

Finnveden G., Johansson J., Lind P., Moberg G. 2005. Life cycle assessment of energy from solid waste—part 1: general methodology and results, J. Clean. Prod. 13,213–229;

Fresner, J., 1998. Cleaner production as a means for effective environmental management, J. Clean. Prod. 6(3,4) 171–179;

Guler U.A., Sarioglu M. 2014. Removal of tetracycline from wastewater using pumice stone: equilibrium, kinetic and thermodynamic studies. J. Environ. Health Sci. Eng.12(1),79;

Jankunaite D., Tichonovas M., Buivydiene D., Radziuniene I., Racys V., Krugly E. 2017. Removal of Diclofenac, Ketoprofen, and Carbamazepine from Simulated Drinking Water by Advanced Oxidation in a Model Reactor. Water, Air, Soil Pollut.,228-353;

Jiang X., Guo Y., Zhang L., Jiang W., Xie R. 2018. Catalytic degradation of tetracycline hydrochloride by persulfate activated with nano Fe^0 immobilized mesoporous carbon. Chem. Eng. J. 341,392-401;

Khandaya W.A., Hameed B.H. 2018. Zeolite-hydroxyapatite-activated oil palm ash composite for antibiotic tetracycline adsorption. Fuel.,215,499–505;

Kurk F., Eagan P. 2008.The value of adding design-for-the-environment to pollution prevention assistance options. J. Clean. Prod. 16,722-726;

Liu P., Liu W.J., Jiang H., Chen J.J., Li W.W., Yu H.Q., 2012.Modification of bio-char derived from fast pyrolysis of biomass and its application in removal of tetracycline from aqueous solution, Bioresour. Technol. 12, 235–240;

López-Peñalver, J.J., Sánchez-Polo, M., Gómez-Pacheco,C.V., Rivera-Utrilla, J. 2010. Photodegradation of tetracyclines in aqueous solution by using UV and UV/H_2O_2 oxidation processes. J Chem Technol Biotechnol. 85, 1325–1333;

Lu T., Zhu Y., Qi Y., Wang W., Wang A. 2018. Magnetic chitosan–based adsorbent prepared via Pickering high internal phase emulsion for high-efficient removal of antibiotics. Int. J. Biol. Macromol.106,870-877;

Ma, J., Sun, Y., Yu, F. 2017. Efficient removal of tetracycline with KOH-activated graphene from aqueous solution. R. Soc. open sci. 4: 170731. http://dx.doi.org/10.1098/rsos.170731;

Martins A.C., Pezoti O., Cazetta A.L., Bedin K.C., Yamazaki D.A.S., Bandoch G.F.G., Asefa T., Visentainer J.V., Almeida V.C. 2015. Removal of tetracycline by NaOH-activated carbon produced from macadamia nut shells: Kinetic and equilibrium studies. Chem. Eng. J.260,291–299;

Morali E.K, Uzal N., Yetis U. 2016. Ozonation pre and post-treatment of denim textile mill effluents: Effect of cleaner production measures, J. Clean. Prod.137, 1-9;

Moussavi G., Khosravi R., 2011. The removal of cationic dyes from aqueous solutions by adsorption onto pistachio hull waste. Chem. Eng. Res. Des.,89 (10),2182–2189;

Naidu, R., Arias Espana V.A., Liu, Y., Jit J., 2016. Emerging contaminants in the environment: risk-based analysis for better management. Chemosphere,154,350-357;

Palm G.J., Lederer T., Orth P., Saenger W., Takahashi M., Hillen W., Hinrichs W. 2008. Specific binding of divalent metal ions to tetracycline and to the repressor/tetracycline complex J. Biol. Inorg. Chem.13,1097–1110;

Petrella, A., Petruzzelli, V., Basile, T., Petrella, M., Boghetich, G., Petruzzelli, D. 2010. Recycled porous glass from municipal/industrial solid wastes sorting operations as a lead ion sorbent from wastewaters, React. Funct. Polym., 70, 203-209;

Petrella A., Cosma P., Rizzi V., De Vietro N. Porous 2017. Alumosilicate Aggregate as Lead Ion Sorbent in Wastewater Treatments. Separations.4(3),25;

Petrella A., Spasiano D., Acquafredda P:, De Vietro N., Ranieri E., Cosma P. Rizzi V., Petruzzelli V., Petruzzelli D. 2018. Heavy metals retention (Pb(II), Cd(II), Ni(II)) from single and multimetal solutions by natural biosorbents from the olive oil milling operations. Process Saf. Environ. Prot. 114,79–90;

Petrie, B., Barden R., Kasprzyk-Hordern B. 2014. A review on emerging contaminants in wastewaters and the environment: current knowledge, understudied areas and recommendations for future monitoring. Water Res.72,3-27;

Qin, Q., Wu, X., Chen, L., Jiang, Z., Xu, Y. 2018. Simultaneous removal of tetracycline and Cu(II) by adsorption and coadsorption using oxidized activated carbon RSC Adv., 8, 1744;

Rizzi V., Longo A., Fini P., Semeraro P., Cosma P., Franco E., García R., Ferrándiz M., Núñez E., Gabaldón J.A., Fortea I., Pérez E., Ferrándiz M. 2014. Applicative Study (Part I): The Excellent Conditions to Remove in Batch Direct Textile Dyes (Direct Red, Direct Blue and Direct Yellow) from Aqueous Solutions by Adsorption Processes on Low-Cost Chitosan Films under Different Conditions. Adv. Chem. Eng. Sci.,4,454-469;

Rizzi V., Fini P., Fanelli F., Placido T., Semeraro P., Sibillano T., Fraix A., Sortino S., Agostiano A., Giannini C., Cosma P. 2016a. Molecular interactions, characterization and photoactivity of Chlorophyll a/chitosan/2-HP-b-cyclodextrin composite films as functional and active surfaces for ROS production. Food Hydrocolloids.58,98-112;

Rizzi V., Fini P., Semeraro P., Cosma P. 2016b. Detailed investigation of ROS arisen from chlorophyll a/Chitosanbased-biofilm. Colloids Surf., B.142,239–247;

Rizzi V., D'Agostino F., Fini P., Semeraro P., Cosma P. 2017a. An interesting environmental friendly cleanup: The excellent potential of olive pomace for disperse blue adsorption/desorption from wastewater. Dyes and Pigm.140,480-490;

Rizzi V., D'Agostino F., Gubitosa J., Fini P., Petrella A., Agostiano A., Semeraro P., Cosma P. 2017b. An Alternative Use of Olive Pomace as a Wide-Ranging Bioremediation Strategy to Adsorb and Recover Disperse Orange and Disperse Red Industrial Dyes from Wastewater Separations,4,29;

Rizzi V., Mongiovì C., Fini P., Petrella P., Semeraro P., Cosma P., 2017c. Operational parameters affecting the removal and recycling of direct blue industrial dye from wastewater using bleached oil mill waste as alternative adsorbent material International Journal of Environment, Agriculture and Biotechnology (IJEAB), 2(4),1560-1572;

Rizzi V., Longo A., Placido T., Fini P., Gubitosa J., Sibillano T., Giannini C., Semeraro P., Franco E., Ferrandiz M., Cosma P. 2018a. A comprehensive investigation of dye–chitosan blended films for green chemistry applications. J. Appl. Polym. Sci.135(10),45945;

Rizzi V., Fiorini F., Lamanna G., Gubitosa J., Prasetyanto E.A., Fini P., Fanelli F., Nacci A., De Cola L., Cosma P, 2018b. Polyamidoamine-Based Hydrogel for Removal of Blue and Red Dyes from Wastewater, Adv. Sustainable Syst., 1700146;

Rizzi,V., Prasetyanto,E.A., Chen, P., Gubitosa,J., Fini,P., Agostiano,A., De Cola,L., Cosma,P. 2019. Amino grafted MCM-41 as highly efficient and reversible ecofriendly adsorbent material for the Direct Blue removal from wastewater Journal of Molecular Liquids 273, 435–446;

Rossi Bautitz, I., Nogueira, R.F.P. Degradation of tetracycline by photo-Fenton process—Solar irradiation and matrix effects. 2007. Journal of Photochemistry and Photobiology A: Chemistry 187, 33–39

Safari G.H., Hoseini M., Seyedsalehi M., Kamani H., Jaafari J., A. H. Mahvi. 2015. Photocatalytic degradation of tetracycline using nanosized titanium dioxide in aqueous solution. Int. J. Environ. Sci. Technol.12,603–616;

Selmi T., Sanchez-Sanchez A., Gadonneix P., Jagiello J., Seffen M., Sammoud H., Celzard A., Fierro V. 2018. Tetracycline removal with activated carbons produced by hydrothermal carbonisation of Agave americana fibres and mimosa tannin. Sep. Purif. Technol. 200,155–163;

Shao L., Ren Z., Zhang G., Chen L. Facile synthesis, characterization of a $MnFe_2O_4$/activated carbon magnetic composite and its effectiveness in tetracycline removal. Mater. Chem. Phys. 2012, 135,16-24;

Sayğılı, H., Güzel, F. 2016, Effective removal of tetracycline from aqueous solution using activated carbon prepared from tomato (Lycopersicon esculentum Mill.) industrial processing waste. Ecotoxicology and Environmental Safety, 131, 22–29;

Song W., Huang M., Rumbeiha W, Li H. 2007. Determination of amprolium carbadox, monensin and tylosin in surface water by liquid chromatography/tandem mass spectrometry. Rapid Commun. Mass Spectrom.21(12),1944-50;

Sophia A.C., Lima E.C., 2018. Removal of emerging contaminants from the environment by adsorption Ecotoxicol. Environ. Saf.150,1–17;

Sousa J.C.G., Ribeiro A.R., Barbosa M.O., Pereira M.F.R., Silva A.M.T. 2018. A review on environmental monitoring of water organic pollutants identified by EU guidelines. J. Hazard. Mater.344,146–162;

Thomas, S.P., Alghamdi, M.N. 2018. Chitosan composites with nanohydroxyapatite prepared by wet chemical reaction along with microwave irradiation: permeability and swelling aspects, Polymer Composites.39(3),718-729.

Vega, E.,Valdes, H. 2018. New evidence of the effect of the chemical structure of activated carbon on the activity to promote radical generation in an advanced oxidation process using hydrogen peroxide Microporous and Mesoporous Materials 259,1-8;

Wen,X., Zeng,Z., Du,C., Huang,D., Zeng,G., Xiao,R., Lai,C., Xu,P., Zhang, C.,Wan,J., Hu,L.,Yin,L., Zhou,C., Deng, R. 2019. Immobilized laccase on bentonite-derived mesoporous materials for removal of tetracycline Chemosphere 222, 865-871;

Yeşilova E., Osman B., Kara A., Özer E.T. 2018. Molecularly imprinted particle embedded composite cryogel for selective tetracycline adsorption. Sep. Purif. Technol.200,155–163;

Zhanga, Z., Lana, H., Liua, H., Qu, J. 2015. Removal of tetracycline antibiotics from aqueous solution by amino-Fe (III) functionalized SBA15. Colloid Surf. A: Physicochem. Eng. Aspects 471, 133–138;

Zhang Y., Zuo S., Zhou M., Liang L., Ren G. 2018. Removal of tetracycline by coupling of flow-through electro-Fenton and insitu regenerative active carbon felt adsorption. Sep. Purif. Technol.200,155–163;

Zhou Y., Yang Q., Zhang D., Gan N., Li Q., Cuan J. 2018. Detection and removal of antibiotic tetracycline in water with a highly stable luminescent MOF. Sens. Actuators, B 262,137–143;

Zhu X., Liu Y., Qian F., Zhou C., Zhang S., Chen J. 2014. Preparation of magnetic porous carbon from waste hydrochar by simultaneous activation and magnetization for tetracycline removal. Bioresour. Technol.154,209–214;

Zilouei H., Abdolmaleki A.Y., Khorasani S.N., Zargoosh K. 2018. Adsorption of tetracycline from water using glutaraldehyde-crosslinked electrospun nanofibers of chitosan/poly (vinyl alcohol). Water Sci. Technol.77(5),1324-1335.